

## Annealing of a glycerol glass: Enthalpy, fictive temperature and glass transition temperature change with annealing parameters

P. Claudy\*, S. Jabrane, J.M. L  toff  

*Laboratoire de Thermochimie Min  rale, UPRES A CNRS 5079, INSA, B  t 401-20 Av. A. Einstein, F-69621 Villeurbanne, France*

Received 14 October 1996; accepted 6 November 1996

### Abstract

The enthalpy change (relaxation enthalpy) of the glycerol glass with annealing time was studied using DSC for different annealing temperatures. The investigation of the fictive temperature and glass transition temperature variations with annealing parameters was also carried out. In this study, a well-annealed glass was used as a reference for the determination of relaxation enthalpy. Two enthalpy contributions to relaxation enthalpy were observed. The results were discussed in terms of a multi-step thermodynamic transformation of molecular associations in the glass transition range. A linear relation was also found between relaxation enthalpy and fictive temperature. This well-known conclusion was established from experimental results. Finally, an empirical relation was proposed for the variation of the fictive temperature with annealing parameters.   1997 Elsevier Science B.V.

**Keywords:** DSC; Enthalpy; Fictive temperature; Glass; Glycerol; Relaxation

### 1. Introduction

Glasses are known to undergo changes with time in their thermodynamic and mechanical properties, when annealed at temperatures below their glass transition temperature  $T_g$ . Enthalpy [1–6] and specific volume [7–9] changes with annealing time and temperature have been particularly studied. Other properties of glasses, such as yield stress and refractive index, are also affected by annealing.

Isothermal enthalpy relaxation is widely described in literature as both nonexponential and nonlinear. Nonexponentiality is mostly accounted for by using the Kolrausch–Williams–Watt (KWW) function. The

latter function is considered to be equivalent to the sum of exponential functions resulting from a distribution of relaxation times around a mean value  $\tau^*$ . For example, B  hr et al. [1] investigated the heat capacity of polybutadiene in the glass transition region after annealing experiments were performed. Isothermal enthalpy relaxation was found to follow a KWW law. In a very recent paper, Mehl [2] studied the isothermal enthalpy relaxation of glycerol and 1,2-propanediol. He also analyzed experimental results using the KWW equation.

Nonlinearity stems from the fact that relaxation depends not only on annealing temperature, but also on the structural state of the vitreous material relative to the so-called ‘equilibrium’ vitreous state. Consequently, relaxation depends on both temperature and supplementary macroscopic thermodynamic variables

\*Corresponding author.

corresponding to the microscopic structural state of glass.

Narayanaswamy [10] and Moynihan [11] expressed the relaxation time as a function of temperature and fictive temperature. Using the Adam–Gibbs [12] configuration entropy theory, Hodge [13] proposed an expression of relaxation time similar in form to the well-known Vogel–Fulcher–Tammann equation.  $\tau^*$  is a function of temperature and fictive temperature. Perez [14] expressed the relaxation time as a function of temperature and ‘defects’ concentration using a model where relaxation is viewed as the collapse of highly disordered sites or ‘defects’.

Other approaches to isothermal relaxation exist in literature. One can cite Bauwens–Crowet and Bauwens [3], who studied the effect of thermal annealing on enthalpy relaxation and yield stress of polycarbonate. The authors propose a theoretical treatment of their results relying on free volume, configuration and activation concepts.

In this paper, isothermal enthalpy relaxation of glycerol will be studied with emphasis on the thermodynamic variables of glass and different enthalpy contributions to glass transition.

## 2. Experimental

### 2.1. Apparatus

Measurements were made using a DSC Mettler TA 2000 B calorimeter. It was calibrated with regard to temperature and heat flow using the temperatures and heats of melting of high purity metals and compounds [15]. The calorimeter was purged with pure and dry argon.

### 2.2. Materials

Glycerol was purchased from Aldrich; its purity was 99.5% by mass. The water content, as determined by Karl Fisher titration, was ca. 0.04% by mass. Handling of glycerol was done in a glove box under a dry inert atmosphere (argon). The samples were sealed in aluminium crucibles (40  $\mu$ l) and weighed inside the glove box. First set of experiments were performed with 40.9 mg sample; and second with 40.3 mg sample.

### 2.3. Procedure

The present study is based on the subtraction of the DSC curves of annealed glasses at a temperature  $T_a < T_g$  during a time  $t_a$  from that of a well annealed reference glass at  $T_{ref}$  during a time  $t_{ref}$ . This choice was preferred to that of an unannealed or quenched glass because it was more likely to lead to less scattered results than those obtained with, for example a quenched glass. Furthermore, the reference state had to be well defined. Note that Mehl [2], who also studied isothermal enthalpy relaxation of glycerol (and 1,2-propanediol), used a 0 min annealed glass as a reference, contrary to ours.

Each run consisted of the following steps –

1. the sample was quenched in liquid nitrogen
2. the sample was placed in the calorimeter previously cooled at the annealing temperature  $T_a$
3. it was kept at  $T_a$  for a time  $t_a$
4. it was cooled from  $T_a$  to 110 K at a cooling rate of 30 K  $\text{min}^{-1}$
5. the DSC curve (of the annealed glass) was recorded between 110 and 240 K using a heating rate of 2 K  $\text{min}^{-1}$
6. the sample was then cooled from 240 K to  $T_{ref}$  at a cooling rate of 30 K  $\text{min}^{-1}$
7. it was kept at  $T_{ref}$  for a time  $t_{ref}$
8. the sample was then cooled from  $T_{ref}$  to 110 K at 30 K  $\text{min}^{-1}$
9. the DSC curve (of the reference glass) was recorded between 110 and 240 K using a heating rate of 2 K  $\text{min}^{-1}$

This protocol had a double aim:

- to use the same sample for obtaining the annealed and reference glasses;
- to leave the sample undisturbed inside the calorimeter in order to reduce experimental scatter due to differences in heat transfer between the calorimeter and the sample.

## 3. Results

### 3.1. DSC curves

The annealing temperatures used were: 153, 158, 163, and 168 K. The annealing times varied from 5 to 160 min.

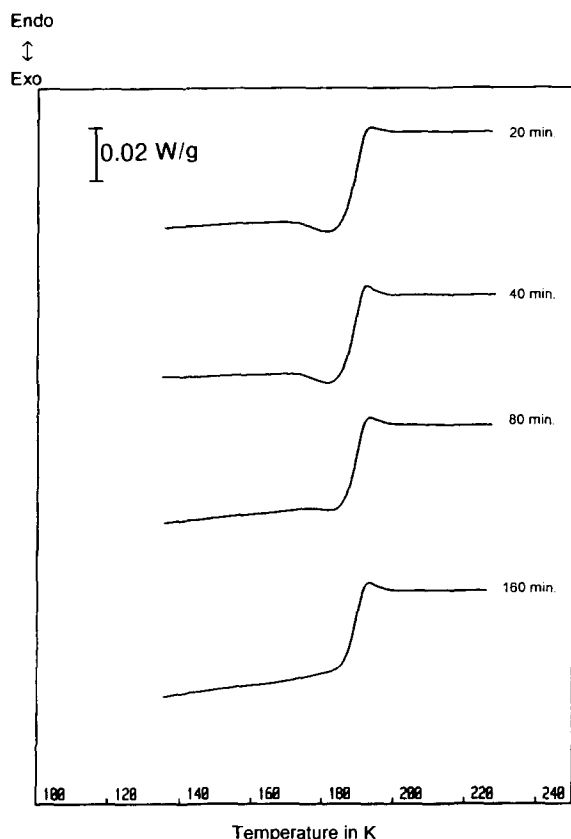


Fig. 1. Changes in DSC curves with annealing time for a sample annealed at 163 K.

The DSC curves of the annealed samples ( $T_a, t_a$ ) showed differences in the glass transition range depending on annealing temperature (the changes for  $T_a=163$  K and  $t_a=20, 40, 80, 160$  min are shown in Fig. 1):

- $T_a=153$  and 158 K: presence of an 'exothermal' effect in the glass transition range (usually associated with quenching) which decreased with annealing time.
- $T_a=163$  K: presence of an 'exothermal' effect which decreased with annealing time to finally disappear for  $t_a=160$  min (Fig. 1).
- $T_a=168$  K: absence of the 'exothermal' effect.

### 3.2. Determination of enthalpy change during annealing

Enthalpy change during annealing was determined by subtracting the DSC curve of the annealed glass

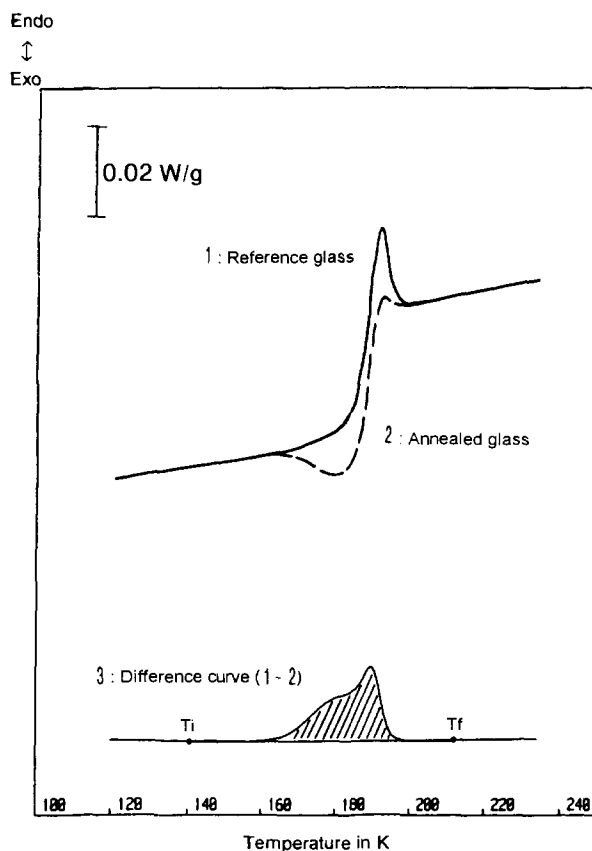


Fig. 2. Determination of relaxation enthalpy. curve 1: DSC curve of the reference glass ( $T_{ref}=173$  K,  $t_{ref}=60$  min); curve 2: DSC curve of an annealed glass ( $T_a=153$  K,  $t_a=80$  min); curve 3: Difference curve  $\Delta W=W_{ref}(T)-W(T)$  between reference glass and annealed glass. The integration of the  $\Delta W$  curves yields the relaxation enthalpy  $\Delta H$ .

( $T_a, t_a$ ) from that of the reference glass ( $T_{ref}, t_{ref}$ ), as is shown in Fig. 2. The reference glass was annealed for 60 min at 173 K. Longer annealing times did not show any significant changes in the DSC curves on heating. Note that the DSC curve of the reference glass presents an important endothermic effect (overshoot) in the glass transition range (curve 1).

Let  $W(T)$  be the calorimetric signal (in  $W g^{-1}$ ) of the annealed glass ( $T_a, t_a$ ) and  $W_{ref}(T)$  that of the reference glass. The integration of the difference curve  $\Delta W(T)=W_{ref}(T)-W(T)$  (curve 3) yielded the enthalpy change:

$$\Delta H = - \int_{T_i}^{T_f} \Delta W(T) dT. \quad (1)$$

This enthalpy corresponds to the difference in enthalpy states between the annealed glass ( $T_a, t_a$ ) and the reference glass ( $T_{ref}, t_{ref}$ ), the latter representing a quasi-equilibrium state. Because the enthalpy change during annealing was determined on heating, it is clear that the shaded area in curve 3 (Fig. 2) corresponds to an enthalpy effect in the glass transition range upon heating (its sign is opposite to the change in enthalpy during annealing).

### 3.3. $\Delta W$ curves

The variations in  $\Delta W$  curves with annealing parameters are summarized in Fig. 3.  $\Delta W$  curves exhibited two enthalpy effects: the first effect is associated with the 'exotherm' in the DSC curves of glasses annealed at  $T_a < 168$  K (see the construction of  $\Delta W$  curves in Fig. 2), and the second (main) effect. The graphic separation into two effects was simply done by sub-

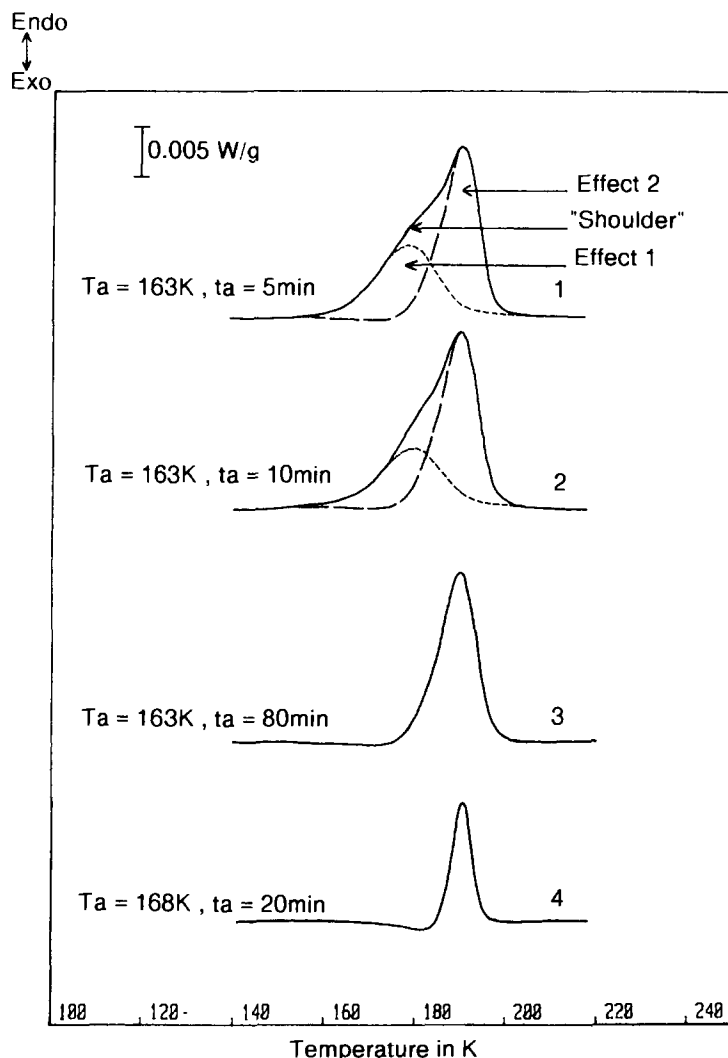


Fig. 3. Variations in  $\Delta W$  curves (difference between DSC curves of reference glass and annealed glass) with annealing parameters. Two contributions are observed: a first effect (effect 1) and a second (main) effect (effect 2). The decomposition into two effects is achieved by subtracting the  $\Delta W$  curve corresponding to  $T_a=163$  K,  $t_a=80$  min (curve 3) from the  $\Delta W$  curves showing a 'shoulder'.

tracting  $\Delta W$  curves showing a 'shoulder' from the  $\Delta W$  curve corresponding to  $T_a=163$  K,  $t_a=80$  min (curve 3 in Fig. 3).

In a first step (Fig. 3), the first effect decreased with annealing time while the amplitude of the second effect remained practically unaffected. This was then followed, in a second step, by the decrease of the second (main) effect for longer annealing times. It thus appears that the first effect is a preliminary step to the second enthalpy effect. Finally, all samples annealed at 168 K exhibited one apparent effect only (second effect). This implies that the first effect has taken place in annealing times shorter than the shortest used (i.e., for  $t < 5$  min).

### 3.4. Dependence of enthalpy change on annealing parameters

Enthalpy variation data are plotted as a function of annealing time for different annealing temperatures in Fig. 4.  $\Delta H=0$  corresponds to the reference glass. The value of  $\Delta H$  for a quenched sample ( $t_a=0$  min), evaluated as  $-10.43$  J g<sup>-1</sup> is also plotted on the same figure. The results are summarized in Table 1. The most important feature of Fig. 4 is that the enthalpy decreases more rapidly (in absolute value) with annealing time, when annealing temperatures are higher. Note that most often, the rate of a transforma-

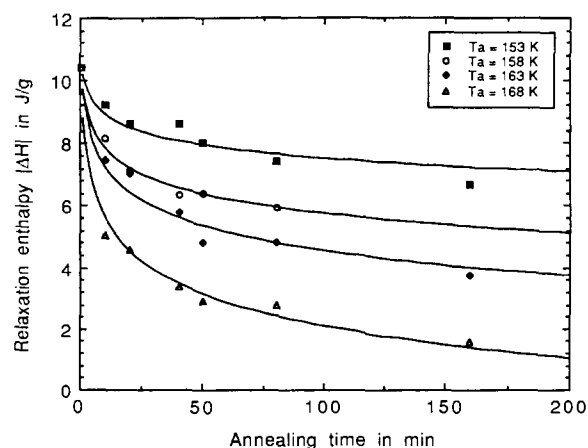


Fig. 4. Variations of relaxation enthalpy with annealing parameters.  $\Delta H=0$  J g<sup>-1</sup> corresponds to the reference glass.  $H=-10.43$  J g<sup>-1</sup> corresponds to a quenched glass.

Table 1  
Relaxation enthalpy  $\Delta H$  vs. annealing parameters ( $T_a$ ,  $t_a$ )

| $t_a$ (min) | $\Delta H$ (J g <sup>-1</sup> ) |             |             |             |
|-------------|---------------------------------|-------------|-------------|-------------|
|             | $T_a=153$ K                     | $T_a=158$ K | $T_a=163$ K | $T_a=168$ K |
| 10          | -9.21                           | -8.16       | -7.47       | -5.04       |
| 20          | -8.61                           | -7.15       | -7.06       | -4.57       |
| 40          | -8.64                           | -6.37       | -5.79       | -3.37       |
| 50          | -8.02                           | -6.41       | -4.82       | -2.94       |
| 80          | -7.39                           | -5.91       | -4.80       | -2.76       |
| 160         | -6.69                           |             | -3.74       | -1.59       |

tion increases with temperature, the opposite being a rare occurrence.

Enthalpy variation data were analyzed using a KWW function as in [2]:

$$\Omega = \frac{H(t) - H(\infty)}{H(0) - H(\infty)} = \exp \left[ -\left( \frac{t}{\tau^*} \right)^\beta \right] \quad (2)$$

The values of  $\beta$  and of  $\tau^*$  giving the best fit are shown in Figs. 5 and 6, respectively, as a function of annealing temperature. Note that the values of  $\beta$  obtained are similar to those given by Mehl [2], in an annealing temperature range close to ours.

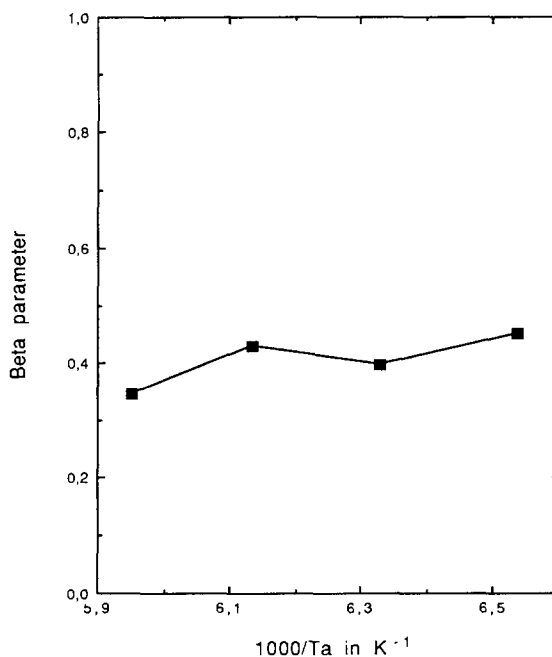


Fig. 5. Parameter  $\beta$  as a function of  $1000/T_a$  (Eq. (2)).

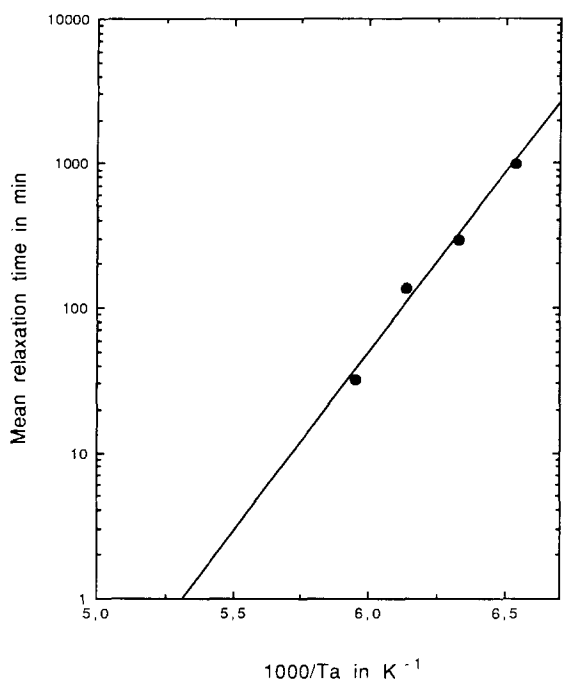


Fig. 6. Mean relaxation time  $\tau^*$  as a function of  $1000/T_a$  (Eq. (2)).

### 3.5. Variation of fictive temperature with annealing parameters

A number of steps are required to calculate  $T_{\text{fic}}$  from Eq. (3), given by Flynn [16] (and also by Moynihan [17]):

$$\int_{T_4}^{T_{\text{fic}}} (C_{p_l} - C_{p_g}) dT = \int_{T_4}^{T_2} (C_p - C_{p_g}) dT \quad (3)$$

with

$C_{p_l}$ : heat capacity of the liquid

$C_{p_g}$ : heat capacity of the glass below the glass transition range

$T_{\text{fic}}$ : fictive temperature

$T_2$ : a temperature below the glass transition range

$T_4$ : a temperature above the glass transition range (liquid)

The steps required to calculate  $T_{\text{fic}}$  are as follows:

1. computation of the heat capacity  $C_p$  of glass below the glass transition range. It was taken as a linear function of temperature using a least squares

Table 2  
Fictive temperature as a function of annealing parameters \*

| $t_a$ /(min) | $T_a=153$ K | $T_a=158$ K | $T_a=163$ K | $T_a=168$ K |
|--------------|-------------|-------------|-------------|-------------|
| 10           | 191.7       | 190.3       | 189.7       | 187.8       |
| 20           | 191.6       | 190.7       | 189.4       | 186.8       |
| 40           | 190.7       | 189.1       | 188.1       | 185.4       |
| 50           | (193.6)     | 189.6       | 187.9       | 185.9       |
| 80           | 190.4       | 189.1       | 186.7       | 184.2       |
| 160          | 189.8       |             | 185.6       | 183.1       |

\*  $T_{\text{fic}}$  of the reference glass (annealed at 173 K for 60 min) is 181.6 K (mean value).  $T_{\text{fic}}$  of the quenched glass is 196.0 K.

fitting between  $T_1=130$  K and  $T_2=150$  K. These temperatures were chosen well below the glass transition.

2. computation of  $\int_{T_4}^{T_2} (C_p - C_{p_g}) dT$  between  $T_2=130$  K and  $T_4=225$  K.
3. the enthalpy curve of the liquid was fitted with a first order polynomial using  $T_3=205$  K and  $T_4=225$  K. These temperatures were chosen well above the glass transition.
4.  $T_{\text{fic}}$  was taken as the intersection of the enthalpy curve of the liquid and that of the glass below the glass transition range.

The fictive temperatures of the annealed glasses ( $T_a$ ,  $t_a$ ) are given in Table 2. The mean fictive temperature of the reference glass was determined as 181.6 K. The fictive temperature of a quenched glass was determined as 196.0 K. Fig. 7 plot the function  $(T_{\text{fic}} - T_a)$  vs. the Napierian logarithm of annealing time  $t_a$  (in seconds) for the annealed glasses ( $T_a$ ,  $t_a$ ). This representation has the advantage of expressing the fictive temperature of the annealed glass relative to the annealing temperature  $T_a$  which also represents the so-called theoretical 'equilibrium' fictive temperature  $T_{\text{fic}}(\infty) = T_a$ . Note that  $T_{\text{fic}}(\infty)$  is a theoretical temperature, whereas the fictive temperature of the reference glass (which can be considered as a quasi-equilibrium metastable vitreous state), estimated as 181.6 K, was calculated from experimental heat capacity curves. The experimental isotherms in Fig. 7 are appreciably linear. It is clear, however, that they are not parallel to one another. Indeed, the rate of change of the fictive temperature is slightly quicker when the annealing temperature is higher. Finally, it should be noted that the isochronal difference between two

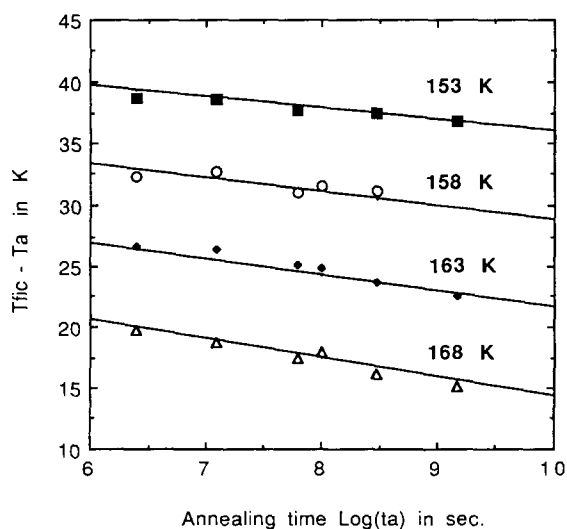


Fig. 7. Change of fictive temperature with annealing time for the different annealing temperatures: (■) 153 K, (○) 158 K, (◆) 163 K, (△) 168 K. The calculated isotherms using Eq. (4) in the text are drawn in full lines.

consecutive isotherms is roughly equal to the relative annealing temperature difference.

From the linearity of the experimental isotherms in Fig. 7, one can write:

$$T_{\text{fic}} = a' \log(t_a) + c$$

where  $a'$  is a function of annealing temperature (since the isotherms are not parallel). It is assumed that the coefficient  $a'$  is a linear function of annealing temperature (in the limit of the studied annealing temperature range):

$$a' = aT_a + b$$

hence, the following relation for the variation of fictive temperature with annealing parameters ( $T_a$ ,  $t_a$ ) for  $T_{\text{fic}} > T_{\text{fic(ref)}}$ :

$$T_{\text{fic}} = [aT_a + b] \log(t_a) + c \quad (4)$$

the best fit (using the least squares method) was found for:

$$a = -0.04509, \quad b = 6.008, \quad c = 198.03$$

The agreement between calculated fictive temperature using Eq. (4) and experimental fictive temperature is good, the largest relative error ( $(T_{\text{fic}} - T_{\text{fic(cal)}})/T_{\text{fic}}$ )

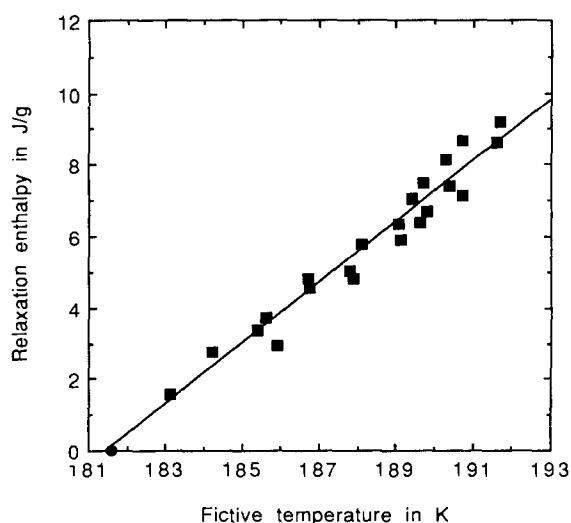


Fig. 8. Relaxation enthalpy vs. fictive temperature for all annealed glasses (■).  $\Delta H = 0 \text{ J g}^{-1}$  corresponds to the reference glass ( $T_{\text{fic}} = 181.6 \text{ K}$  (●)). The graph is appreciably linear with a slope of  $0.85 \text{ J K}^{-1} \text{ g}^{-1}$ . This value is equal to  $\Delta C_p$  at the glass transition in the limit of experimental errors.

$T_{\text{fic}}$ ) being 0.33%. Eq. (4) must however be considered as an empirical relation rather than a kinetic equation (in its derived form).

Note that the fitting parameter  $c = 198.03$  corresponds to the fictive temperature of a 1 s annealed glass; in other words, to an almost perfectly quenched glass. The latter temperature is not very different from the experimental fictive temperature of a quenched glass ( $T_{\text{fic}} = 196.0 \text{ K}$ ).

### 3.6. Relation between enthalpy change and fictive temperature

Enthalpy change data are plotted as a function of fictive temperature in Fig. 8. The graph is appreciably linear with a slope of  $0.85 \text{ J K}^{-1} \text{ g}^{-1}$ . The mean  $\Delta C_p$ , in this work, was estimated as  $0.90 \text{ J K}^{-1} \text{ g}^{-1}$ . This value is to be compared to the mean value of  $\Delta C_p$ , found in literature and calculated as  $0.85 \text{ J K}^{-1} \text{ g}^{-1}$  [18–22]. It is therefore possible to write within the limit of experimental errors:

$$\Delta H \equiv \Delta C_p (T_{\text{fic(ref)}} - T_{\text{fic}}) = \Delta C_p \Delta T_{\text{fic}} \quad (5)$$

Note that a similar relation was given by Bauwens–Crowet and Bauwens in [3] where, instead of the

'usual' fictive temperature, a structural temperature  $\theta$  is used. The latter temperature is calculated using a differential equation which stems from free volume and activation concepts. It should be noted that the fictive temperature can be a very practical way of calculating  $\Delta H$  provided  $\Delta C_p$  is known with high precision. This is difficult in practice, since  $\Delta C_p$  appreciably depends on the choice of baselines used to calculate its value. When  $\Delta C_p$  is known with great accuracy, the determination of  $T_{\text{fic}}$  should enable in getting around the difficulty of directly calculating  $\Delta H$ , since the latter quantity involves the subtraction of the heat capacity curve of the annealed glass from a reference glass.

### 3.7. Glass transition temperature

Two choices were made for the determination of the glass transition temperature  $T_g$ :

1.  $T_{g(\text{inflection})}$ , the inflection point of the change in the calorimetric signal associated with the glass transition;

Table 3  
Inflection point glass transition temperature vs. annealing parameters ( $T_a$ ,  $t_a$ )

| $t_a$ (min) | $T_{g(\text{inflection})}$ (K) |             |             |             |
|-------------|--------------------------------|-------------|-------------|-------------|
|             | $T_a=153$ K                    | $T_a=158$ K | $T_a=163$ K | $T_a=168$ K |
| 10          | 189.2                          | 189.0       | 189.0       | 189.1       |
| 20          | 188.7                          | 189.0       | 189.4       | 188.9       |
| 40          | 189.0                          | 189.1       | 188.9       | 188.9       |
| 50          | 189.3                          | 189.3       | 189.3       | 189.3       |
| 80          | 188.9                          | 189.3       | 189.4       | 189.1       |
| 160         | 188.9                          |             | 189.3       | 188.8       |

Table 4  
Midpoint glass transition temperature vs. annealing parameters ( $T_a$ ,  $t_a$ )

| $t_a$ (min) | $T_{g(\text{midpoint})}$ (K) |             |             |             |
|-------------|------------------------------|-------------|-------------|-------------|
|             | $T_a=153$ K                  | $T_a=158$ K | $T_a=163$ K | $T_a=168$ K |
| 10          | 188.2                        | 188.1       | 188.3       | 188.1       |
| 20          | 188.2                        | 188.4       | 188.7       | 187.8       |
| 40          | 188.2                        | 188.2       | 188.3       | 187.7       |
| 50          | 188.9                        | 188.6       | 188.6       | 187.9       |
| 80          | 188.2                        | 188.6       | 188.7       | 187.3       |
| 160         | 188.2                        |             | 188.7       |             |

2.  $T_{g(\text{midpoint})}$  the midpoint of the calorimetric signal associated with the glass transition.

The data are given in Tables 3 and 4, respectively, as a function of annealing parameters. The results showed that the glass transition temperature, for both choices, did not vary in a significant way with annealing time, whatever the annealing temperature be. The mean value of  $T_{g(\text{inflection})}$  is 189.1 K and the mean value for  $T_{g(\text{midpoint})}$  is 188.3 K.

## 4. Discussion

### 4.1. Thermodynamic variables of glass

This study shows that the isothermal enthalpy relaxation of glycerol involves two enthalpic contributions  $\Delta H_1$  and  $\Delta H_2$  (the first and the second effects, respectively, in Fig. 3). As a consequence, the application of the KWW equation (Eq. (2)) to isothermal enthalpy relaxation appears to be questionable. Indeed, the KWW equation involves one mean relaxation time  $\tau^*$ , whereas experimental results show that at least two mean relaxation times (i.e. two distributions of relaxation times) are necessary to correctly describe the enthalpy relaxation of glass within the framework of the KWW equation. Furthermore, the  $\beta$  parameter appears to be a fitting parameter rather than the one with a physical meaning. Finally, a stretched exponential is one among many ways of fitting enthalpy relaxation data.

Note that Mehl [2], in his study of relaxation enthalpy of glycerol, observed one enthalpy effect only (main effect), because of the experimental protocol used by this author. Indeed, samples in [2] were cooled to 113 K at 10 K min<sup>-1</sup> and then warmed at 10 K min<sup>-1</sup> to the annealing temperature, where they were annealed (DSC curves were recorded on heating after cooling back to 113 K at 10 K min<sup>-1</sup>). In our case, the samples were quenched in liquid nitrogen and then placed in the calorimeter, previously cooled at  $T_a$ , where they were annealed. As a consequence, the first enthalpy effect, which was observed in our case, had already taken place in Mehl's experiments during cooling at 10 K min<sup>-1</sup> (a rate relatively much slower than quenching in liquid nitrogen) and the subsequent heating to  $T_a$  at the same rate. This



explains why the maximum relaxation enthalpy obtained in this work is ca.  $-10.5 \text{ J g}^{-1}$  (Fig. 4), whereas it is ca.  $-6 \text{ J g}^{-1}$  in [2].

In the rest of this section, we will qualitatively discuss on the thermodynamic variables of glass and the different thermodynamic contributions to glass transition.

In view of the existence of two enthalpy contributions to enthalpy relaxation, the total differential of enthalpy at constant pressure should be expressed as:

$$dH = \left(\frac{\partial H}{\partial T}\right)_{p,\xi_1,\xi_2} dT + \left(\frac{\partial H}{\partial \xi_1}\right)_{p,T,\xi_2} d\xi_1 + \left(\frac{\partial H}{\partial \xi_2}\right)_{p,T,\xi_1} d\xi_2, \quad (6)$$

where one can think of  $\xi_1$  and  $\xi_2$  as the extent of transformations of a two-step transformation, taking place during annealing. Using the formalism of Prigogine and Defay [23], the apparent heat capacity of glass at constant pressure is thus the sum of two terms (from Eq. (6)):

$$C_p = \left(\frac{dH}{dT}\right)_p = \left(\frac{\partial H}{\partial T}\right)_{p,\xi_1,\xi_2} + \Delta_1 H_{p,T,\xi_2} \left(\frac{d\xi_1}{dT}\right)_{p,\xi_2} + \Delta_2 H_{p,T,\xi_1} \left(\frac{d\xi_2}{dT}\right)_{p,\xi_1}, \quad (7)$$

where:

- term (1),  $C_{p,\xi} = \left(\frac{\partial H}{\partial T}\right)_{p,\xi_i}$ , is the heat capacity at constant  $p$  and  $\xi_i$  or 'true' heat capacity. It depends only on temperature.
- term (2),  $\sum_i \Delta_i H_{p,T,\xi_i} = \left(\frac{d\xi_i}{dT}\right)_{p,\xi_j}$ , is the 'configurational' heat capacity and  $\Delta_i H_{p,T,\xi_i} = \left(\frac{\partial H}{\partial \xi_i}\right)_{p,T,\xi_j}$  the enthalpy of the transformation characterized by  $\xi_i$  at constant  $p$ ,  $T$  and  $\xi_j$ .

The configurational heat capacity (term 2) is linked to the total enthalpy effect:

$$\Delta H_{p,T} = \Delta_1 H_{p,T,\xi_2} + \Delta_2 H_{p,T,\xi_1}. \quad (8)$$

$\Delta H_{p,T}$  (Eq. (8)) also corresponds to an enthalpic effect taking place at the glass transition and represented by the shaded area on curve 3 in Fig. 2. Its relative sign would be positive on heating and negative on cooling or annealing. Finally, because the variation of the extent of a transformation with temperature  $\left(\frac{d\xi_i}{dT}\right)$

can be written as:

$$\left(\frac{d\xi_i}{dT}\right) = \left(\frac{d\xi_i}{dt}\right) \left(\frac{dt}{dT}\right), \quad (9)$$

the dependence on time (kinetics) is thus introduced. The simplest way of expressing  $\left(\frac{d\xi_i}{dt}\right)$  in chemical kinetics is:

$$\left(\frac{d\xi_i}{dt}\right) = f(\xi_i)k(T). \quad (10)$$

Note that the relaxation times in chemical kinetics are a function of  $\xi_i$  and temperature, hence a *nonlinear behaviour*.

A previous study in the laboratory [22] on the glass transition of glycerol by step heating DSC has shown that the observed apparent heat capacity in the glass transition range is indeed the sum of two terms, as in Eq. (7):

- change in *true* heat capacity from that of the liquid to that of glass (below the glass transition range) on cooling (or the opposite on heating)
- a temperature and time dependent *enthalpy effect* (excess or configurational heat capacity), very likely due to molecular associations.

A simulation of the calorimetric signal, in good agreement with experimental results, was made assuming the following equilibrium transformation of molecular associations in the glass transition range:



with  $A_n$  associations or clusters of the  $A$  species ( $A$  representing, as for example, molecule of glycerol). It is the *formation* (cooling) and *destruction* (heating) of the associated species that involves an *enthalpy effect*. In this view, the concentration (or size) of associated species (clusters) in the glass transition range on cooling would be such that the congealing of the structure of the liquid occurs, leading to the formation of a solid (glass) at lower temperatures (this would explain the change of true heat capacity, from liquid to that of a solid since degrees of freedom have been frozen in). On heating, the progressive destruction of these molecular associations takes place in the glass transition range. Note that the idea of molecular organizations in the vitreous state was already introduced by Tammann in 1933 [24] and more recently by

Hoare [25]. The latter author advanced the idea that the glass transition on heating could correspond to the ‘melting’ of clusters present in the vitreous state. A recent study by Jabrane et al. [26] on the application of Van Laar type equations to the composition dependence of  $T_g$  reinforced this view.

The results in this paper, where ‘dynamic’ (not quasi-static) DSC was used suggest that a two-step transformation (rather than a one-step transformation as in Eq. (11)) ought to be considered to account for experimental results. A modelling of enthalpy relaxation and glass transition using a two-step transformation is currently under way. Moreover, a two-step transformation seems reasonable in explaining the well-known enthalpy ‘cross over’ experiments [6].

#### 4.2. Fictive temperature

From Eq. (5), it can be deduced that the fictive temperature is expressed in terms of temperature of enthalpy change. Consequently, the fictive temperature is a mean parameter representing, in terms of temperature, the supplementary thermodynamic variables,  $p$  and  $T$  that are necessary for a correct thermodynamic description of glass. These supplementary variables are the extent of transformations  $\xi_1$  and  $\xi_2$  of the two-step (at least) transformation of molecular associations, taking place in the glass transition range during the thermal treatment of annealing. On a microscopic level, the complexity of the molecular processes may be such that, very likely, there exists a distribution of molecular mechanisms (two distributions, in fact, since two rates of transformation are needed for a correct description of glass).

#### 4.3. Experimental thermodynamic functions

Fig. 9 shows the heat capacity, enthalpy and entropy curves of two glasses with different thermal histories: a glass annealed at 158 K for 20 min (curve 1) and the reference glass, annealed at 173 K for 60 min (curve 2). In Fig. 9(b), the enthalpy curves of both glasses determined from the heat capacity curves:  $H_T^0 = H_{T_0}^0 + \int_{T_0}^T C_p dT$  are shown. Since it is widely accepted that the enthalpy of the liquid does not depend on time,  $T_0$  and  $H_{T_0}^0$  were chosen as arbitrary values ( $T_0=220$  K and  $H_{T_0}^0 = 100$  J g<sup>-1</sup>). Fig. 9(c) shows the entropy curves of both glasses

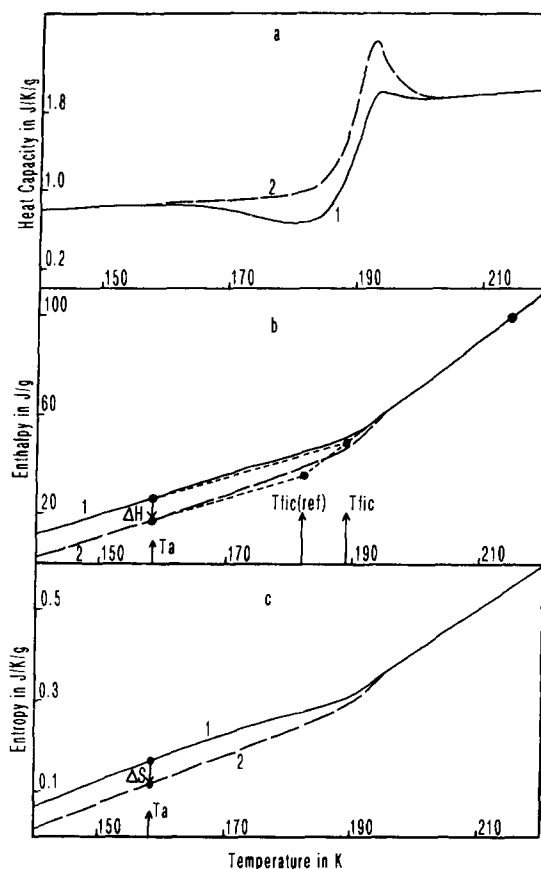


Fig. 9. (a) Heat capacity (in J g<sup>-1</sup> K<sup>-1</sup>), (b) enthalpy (in J g<sup>-1</sup>), and (c) entropy (in J g<sup>-1</sup> K<sup>-1</sup>) curves of an annealed glass at  $T_a=158$  K for 20 min (curve 1) and of the reference glass annealed at 173 K for 60 min (curve 2). In (b),  $\Delta H$  is the relaxation enthalpy,  $T_{fic(ref)}$  the fictive temperature of the reference glass and  $T_{fic}$  the fictive temperature of the annealed glass. In (c),  $\Delta S$  is the relaxation entropy (see text for the determination of enthalpy and entropy curves from heat capacity curves).

determined from the heat capacity curves:  $S_T^0 = S_{T_0}^0 + \int_{T_0}^T (C_p/T) dT$ . As for the enthalpy, the entropy of the liquid does not depend on time.  $T_0$  and  $S_{T_0}^0$  were chosen as 220 K and 0.6 J K<sup>-1</sup> g<sup>-1</sup>, respectively. The difference of enthalpy  $\Delta H_T^0$  and entropy  $\Delta S_T^0$  between the annealed glass ( $T_a, t_a$ ) and the reference glass are illustrated in Fig. 9(b,c) respectively. Fig. 9(c) clearly shows that the entropy of the glycerol glass decreases with annealing. Consequently, the organization in the vitreous state increases with annealing. This is in agreement with

the formation of molecular associations in the vitreous state.

## 5. Conclusion

Enthalpy change of the glycerol glass during annealing involves two enthalpy contributions: a first and a second (main) enthalpy effect. The well-known ‘exotherm’ in DSC curves (which stems from relatively rapid cooling rates) is the manifestation of the first enthalpy effect. It appears that the molecular processes associated with the first enthalpy effect are a preliminary step to those corresponding to the second enthalpy effect. These results are to be correlated to the frequency dependent  $\alpha$  and  $\beta$  relaxation processes. Therefore, in addition to pressure and temperature, at least two supplementary macroscopic thermodynamic variables are necessary for a correct description of the studied glass. We believe that these variables are the extent of reactions of a multi-step molecular transformation in the glass transition range. This transformation is temperature and time dependent, and is most probably due to the molecular associations.

A linear relation was also found between fictive temperature and enthalpy change after annealing experiments were performed. This well-known result was established from the experimental results of this study. The fictive temperature is, consequently, the expression in terms of temperature of relaxation enthalpy. As a result, the fictive temperature is a mean parameter which expresses in terms of temperature, the variables supplementary to pressure and temperature that are necessary for a correct description of the vitreous state, i.e.  $T_{\text{fc}} = f(\xi_1, \xi_2)$ .

## References

- [1] M. Bähr, F. Schreier, J. Wosnitza, H.V. Löhneysen, C. Zhu., X. Qin, H. Chen, X. Liu and X. Wu, *Europhys. Lett.*, 22(6) (1993) 443.
- [2] P.M. Mehl, *Thermochim. Acta*, 272 (1996) 201.
- [3] C. Bauwens-Crowet and J.C. Bauwens, *Polymer*, 23 (1982) 1599.
- [4] G. Vigier and J. Tatibouet, *Polymer*, 34(20) (1993) 4257.
- [5] J.M.G. Cowie and R. Ferguson, *Polymer*, 34(10) (1993) 2135.
- [6] K. Hofer, J. Perez and G.P. Johari, *Philosophical Magazine Lett.*, 64(1) (1991) 37.
- [7] A.J. Kovacs, *J. Polymer Science*, 30 (1958) 131.
- [8] L.C.E. Struik, *Physical Ageing in Amorphous Polymers and Other Materials*, Elsevier, Amsterdam (1978).
- [9] H.H. D Lee and F.J. McGarry, *Polymer*, 34(20) (1993) 4267.
- [10] O.M. Narayanaswamy, *J. Am. Ceram. Soc.*, 54 (1971) 491.
- [11] C.T. Moynihan, A.J. Easteal and M.A. DeBolt, *J. Am. Cer. Soc.*, 59(1-2) (1976) 12.
- [12] G. Adam and J. H Gibbs, *J. Chem. Phys.*, 43 (1965) 139.
- [13] I.M. Hodge, *J. Non Cryst. Solid.*, 131-133 (1991) 435.
- [14] J. Perez, *Polymer*, 29 (1988) 483.
- [15] P. Claudy, B. Bonnetot, G. Chahine and J. M Létouffé, *Thermochim. Acta*, 38 (1980) 75.
- [16] J.H. Flynn, *Thermochim. Acta*, 8 (1974) 69.
- [17] C.T. Moynihan, A.J. Easteal and M.A. DeBolt, *J. Am. Cer. Soc.*, 59(1-2) (1976) 12.
- [18] G.E. Gibson and W.F. Giauque, *J.A.C.S.*, 45 (1923) 93.
- [19] R.O. Davies and G.O. Jones, *Acta. Physica*, 2 (1953) 370.
- [20] W. Kauzmann, *Chem. Rev.*, 48 (1948) 219.
- [21] D. Harran, PhD, Contribution à l'étude thermodynamique des solutions aqueuses qui vitrifient à basses températures, Université de Pau (1976) p.146.
- [22] P. Claudy, J.C. Commerçon and J.M. Létouffé, *Thermochim. Acta*, 128 (1988) 251.
- [23] I. Prigogine and R. Defay, *Thermodynamique chimique*, Vol. I-II, Desoer, Liège, Belgium (1950) pp. 304–307.
- [24] G. Tammann, *Der Glaszustand*, Section IV, 12, Leopold Voss, Leipzig (1933).
- [25] M. Hoare, *Ann. New York Academy Sci.*, 279 (1976) 187.
- [26] S. Jabrane, J.M. Létouffé, and P. Claudy, *Thermochim. Acta*, accepted 5 July (1996).